Structure of AlSb(001) and GaSb(001) surfaces under extreme Sb-rich conditions

Jeffery Houze, Sungho Kim, and Seong-Gon Kim*

Department of Physics and Astronomy, Mississippi State University, Mississippi State, Mississippi 39762, USA
and Center for Advanced Vehicular Systems, Mississippi State University, Mississippi State, Mississippi 39762, USA

S. C. Erwin and L. J. Whitman

Naval Research Laboratory, Washington, DC 20375, USA

We use density-functional theory to study the structure of AlSb(001) and GaSb(001) surfaces. Based on a variety of reconstruction models, we construct surface stability diagrams for AlSb and GaSb under different growth conditions. For AlSb(001), the predictions are in excellent agreement with experimentally observed reconstructions. For GaSb(001), we show that the previously proposed model accounts for the experimentally observed reconstructions under Ga-rich growth conditions but fails to explain the experimental observations under Sb-rich conditions. We propose a model that has a substantially lower surface energy than all $(n \times 5)$-like reconstructions proposed previously and that, in addition, leads to a simulated scanning tunneling microscopy image in better agreement with experiment than existing models. However, this model has higher surface energy than some of (4×3)-like reconstructions, models with periodicity that has not been observed. Hence, we conclude that the experimentally observed (1×5) and (2×5) structures on GaSb(001) are kinetically limited rather than at the ground state.

I. INTRODUCTION

The surfaces and interfaces of III-V semiconductors constitute some of the most important components of the semiconductor industry. For example, III-V heterostructure quantum wells are key components in a wide range of optical and high-frequency electronic devices, including field-effect transistors,[1] resonant tunneling structures,[2] infrared lasers,[3] and infrared detectors.[4] Many of these devices require extremely sharp and clean interfaces. For this reason, an understanding of the atomic-scale morphology of III-V semiconductor surfaces is critical for controlling the growth and formation of their interfaces.[5,6]

It is generally accepted that the surfaces of III-V semiconductors should reconstruct in such a way that the number of electrons is exactly enough to doubly occupy all orbitals on electronegative (V) atoms, leaving all orbitals on electropositive (III) atoms unoccupied. This guiding principle, known as the electron-counting model (ECM), has been used to screen candidate structural models of many observed reconstructions on the surfaces of III-V semiconductors.[7–11] In practice, however, not all experimentally realized reconstructions follow this principle. For example, under Sb-rich growth conditions, GaSb(001) forms surface reconstructions that are weakly metallic and hence violate the ECM,[12] even though the closely related AlSb(001) surface forms insulating reconstructions that satisfy it.[13] The nature of reconstructions that violate the ECM and the underlying reasons for their stability are thus important for understanding III-V surfaces in general.

In this paper, we explore theoretically a large number of judiciously chosen candidate reconstructions on GaSb(001) and AlSb(001). We find that as the growth conditions are varied between Sb-poor and Sb-rich, the predicted sequence of stable reconstructions for GaSb(001) is exactly analogous to those of AlSb(001). Experimentally, however, the picture

is more complicated. In the Sb-poor limit, the observed GaSb(001) reconstruction is indeed analogous to that of AlSb(001). On the other hand, in the Sb-rich limit, the experimentally observed reconstructions for GaSb(001) and AlSb(001) are different. Moreover, in this limit, the predicted and observed reconstructions are in good agreement only for AlSb(001), while for GaSb(001) there remains an unresolved discrepancy between theory and experiment.

Experimentally, the Sb-terminated AlSb(001) surface evolves through the sequence $\alpha(4 \times 3) \rightarrow \beta(4 \times 3) \rightarrow \gamma(4 \times 3) \rightarrow c(4 \times 4)$ as the growth condition is changed from low Sb flux (or high substrate temperature) to high Sb flux (or low temperature).[13] All of these reconstructions are insulating and are well accounted for by structural models proposed in the literature that satisfy the ECM.

Of particular interest here is the Sb-rich AlSb(001)-$c(4 \times 4)$ reconstruction, analogous to the As-rich GaAs(001)-$c(4 \times 4)$ reconstruction, which is observed on AlSb but not GaSb. In contrast to both AlSb and GaAs, the GaSb(001) surface does not exhibit a stable, insulating $c(4 \times 4)$ reconstruction under similar—or any other—growth conditions. Instead, it forms $(n \times 5)$-like reconstructions.[12,14–17] Structural models proposed in the literature for these $(n \times 5)$-like reconstructions violate, by design, the ECM and consequently are weakly metallic.[12] Simulated scanning tunneling microscopy (STM) images based on (2×10) and $c(2 \times 10)$ models closely resemble the experimental images.[12] As a result, these models have been generally accepted as describing the GaSb(001) surface under Sb-rich growth conditions. Nevertheless, we show below on energetic grounds that these models are unlikely to be correct. Specifically, we find their calculated surface energy to be significantly higher than GaSb(001)-$c(4 \times 4)$ for any plausible value of Sb chemical potential. However, since the
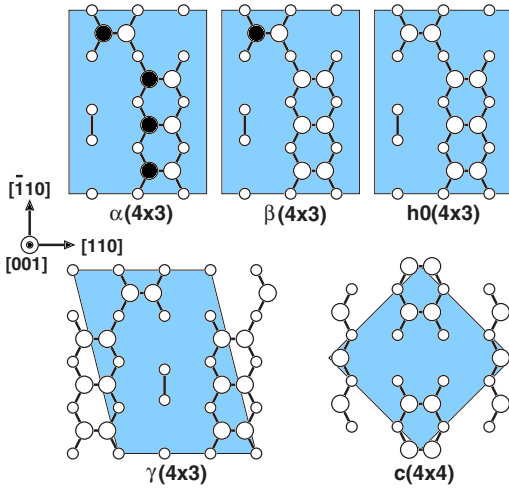
FIG. 1. (Color online) Reconstruction models proposed for the AlSb(001) or GaSb(001) surfaces with (4×3) and (4×4) periodicities. The first two upper layers are shown in a top view. Smaller white circles represent Sb atoms in the top layer of the underlying Sb-terminated AlSb(001) or GaSb(001) surface. Larger circles represent Al or Ga (black) and Sb (white) adatoms. The unit cells are shown in light blue.

experimentally observed reconstruction of GaSb(001) does not have $c(4\times4)$ periodicity, this model cannot be correct either. Thus, a definitive structural model remains to be found.
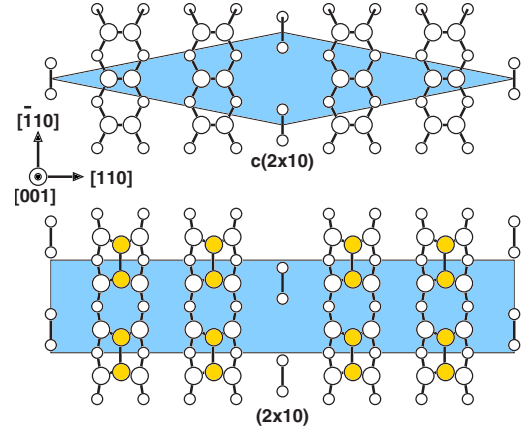

FIG. 2. (Color online) Reconstruction models proposed for the Ga-Sb(001)-(1×5)-like surfaces under the extreme Sb-rich growth condition. See Fig. 1 for color schemes. Gold circles represent second layer Sb adatoms.

II. METHODS

The basic structural models we considered are taken from the literature and are shown in Figs. 1 and 2. Surfaces that satisfy the ECM are generally semiconducting, while those that do not may be metallic. The degree to which a given surface satisfies the ECM can be measured by the excess electron count $\Delta\nu$, which we define here as the difference between the number of available electrons and the number required to satisfy the ECM, per (1×1) surface unit cell.

TABLE I. Electron count for different reconstructions of GaSb(001) surface. The excess electron count per (1×1) surface unit cell is defined as $\Delta\nu=(\tilde{n}-\tilde{m})/A$, where $\tilde{n}$ is the number of available electrons and $\tilde{m}$ is the number of required electrons to satisfy the ECM in the excess of Sb-terminated GaSb(001). A is the area of the surface unit cell in terms of the (1×1) surface unit cell. n_i is the number of adatoms of species i in excess with respect to the Sb-terminated GaSb(001), and $\Theta_i=n_i/A$ is the coverage of adatoms of species i. The relative γ values, in eV per (1×1) surface unit cell, are given with respect to that of $\alpha(4\times3)$.

| Structure	A	n_{III}	n_{V}	Θ_{III}	Θ_{V}	$\Delta\Theta$	$\tilde{n}$	$\tilde{m}$	$\Delta\nu$	γ(Ga rich)	γ(Sb rich)
$\alpha(4\times3)$	12	4	4	0.333	0.333	0.0	62	62	0	0.000	0.000
$\beta(4\times3)$	12	1	7	0.083	0.583	−0.5	68	68	0	0.076	−0.074
$\gamma(4\times3)$	12	0	8	0.0	0.667	−0.667	70	70	0	0.114	**−0.087**
$h0(4\times3)$	12	0	8	0.0	0.667	−0.667	70	70	0	0.118	−0.083
$c(4\times4)$	8	0	6	0.0	0.750	−0.750	50	50	0	0.142	−0.084
$c(2\times10)$	10	0	8	0.0	0.800	−0.800	65	62	0.3	0.255	0.014
(2×10)	20	0	24	0.0	1.200	−1.200	170	164	0.3	0.528	0.166
$s1a$-$c(2\times10)$	10	1	7	0.1	0.700	−0.600	63	62	0.1	0.143	**−0.038**
$s1b$-$c(2\times10)$	10	1	7	0.1	0.700	−0.600	63	62	0.1	0.181	0.000
$s1c$-$c(2\times10)$	10	1	7	0.1	0.700	−0.600	63	62	0.1	0.280	0.099
$s2a$-$c(2\times10)$	10	2	6	0.2	0.600	−0.400	61	62	−0.1	0.137	0.016
$s2b$-$c(2\times10)$	10	2	6	0.2	0.600	−0.400	61	62	−0.1	0.124	0.003
$s2c$-$c(2\times10)$	10	2	6	0.2	0.600	−0.400	61	62	−0.1	0.143	0.023
$s2d$-$c(2\times10)$	10	2	6	0.2	0.600	−0.400	61	62	−0.1	0.141	0.020
$s2e$-$c(2\times10)$	10	2	6	0.2	0.600	−0.400	61	62	−0.1	0.167	0.046
$s2f$-$c(2\times10)$	10	2	6	0.2	0.600	−0.400	61	62	−0.1	0.144	0.023
$s2g$-$c(2\times10)$	10	2	6	0.2	0.600	−0.400	61	62	−0.1	0.182	0.062
$s2h$-$c(2\times10)$	10	2	6	0.2	0.600	−0.400	61	62	−0.1	0.164	0.043
$s2i$-$c(2\times10)$	10	2	6	0.2	0.600	−0.400	61	62	−0.1	0.166	0.045

(a)

(b)
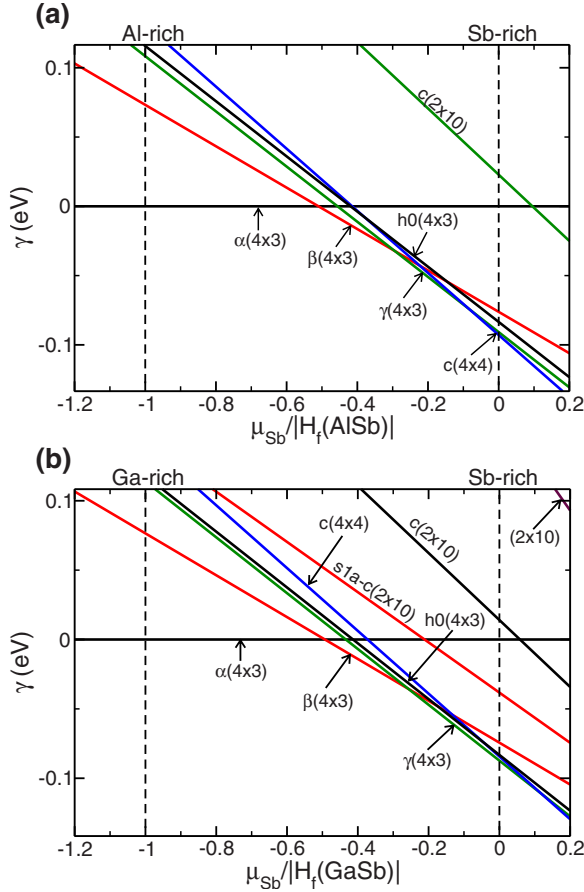
FIG. 3. (Color online) (a) Surface stability phase diagram for AlSb(001) surface. The relative surface energy [Eq. (2)] is plotted as a function of the Sb chemical potential relative to its corresponding bulk value. Dotted vertical lines mark the thermodynamically allowed range of μ_{Sb}. ΔH_f is the heat of formation for AlSb. (b) Surface stability phase diagram for GaSb(001) surface; ΔH_f is the heat of formation for GaSb.

Excess electron counts for the structural models in Figs. 1 and 2 are tabulated in Table I.

To compare the surface energies of reconstruction models with different periodicities and stoichiometries, we consider the surface energy per unit area,

$$\gamma = E_{surf}/A = (E_{tot} - n_{III}\mu'_{III} - n_V\mu'_V)/A, \qquad (1)$$

where E_{tot} is the total energy of a reconstructed surface of area A containing n_{III} group-III and n_V group-V adatoms in excess with respect to the bulk-truncated, Sb-terminated AlSb(001) or GaSb(001). The atomic chemical potentials μ' are more conveniently expressed in terms of excess chemical potentials μ, relative to the energy per atom in the ground-state elemental phases: $\mu' = \mu^{bulk} + \mu$. Assuming the surface to be in thermodynamic equilibrium with the bulk, the III and V chemical potentials are related by $\mu_{III} + \mu_V = \Delta H_f$, where $\Delta H_f = \mu^{bulk}_{III-V} - (\mu^{bulk}_{III} + \mu^{bulk}_V)$ is the formation enthalpy of the bulk III-V crystalline phase[18] (note that ΔH_f is intrinsically negative). Equation (1) can then be rewritten to show more clearly the dependence of γ on the surface stoichiometry and chemical potential:
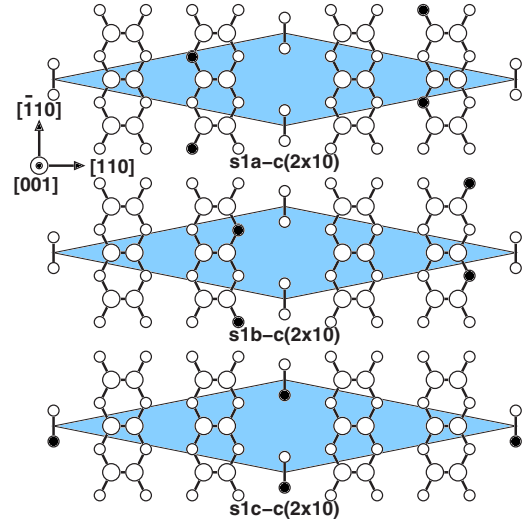

FIG. 4. (Color online) Reconstruction models with a single substitution of Sb atoms by Ga atoms. See Fig. 1 for color schemes.

$$\gamma = \gamma_0 + \mu_V\Delta\Theta. \qquad (2)$$

Here, $\gamma_0 = (E_t - E_{sub}) - \mu^{bulk}_{III-V}\Theta_{III} + \mu^{bulk}_V\Delta\Theta$ is independent of the chemical potentials, and $\Delta\Theta = \Theta_{III} - \Theta_V = (n_{III} - n_V)/A$ is the deviation of the surface stoichiometry from its bulk value. The dependence of γ on chemical potential is given entirely by the second term. Note that μ_V is intrinsically negative and can take values in the range $\Delta H_f \leq \mu_V \leq 0$. Hence, Eq. (2) reflects in a simple way that III-rich reconstructions ($\Theta_{III} > \Theta_V$) are favored under III-rich conditions ($\mu_V \rightarrow \Delta H_f$), V-rich reconstructions ($\Theta_V > \Theta_{III}$) are favored under V-rich conditions ($\mu_V \rightarrow 0$), and for stoichiometric reconstructions ($\Theta_V = \Theta_{III}$), γ does not depend on chemical potential.

To compute the total-energy contribution γ_0 to the surface energy, we performed first-principles calculations using density-functional theory (DFT). The calculations were performed within the local-density approximation[19,20] using ultrasoft pseudopotentials.[21–23] We used a standard supercell technique, modeling the (001) surface with a slab consisting of four bilayers and 10 Å of vacuum. Atoms in the bottom bilayer were fixed at their bulk positions, while all other atoms are allowed to relax until the rms force was less than 0.005 eV/Å. The bottom layer (either Ga or Al) was passivated with pseudohydrogen. A plane-wave cutoff of 300 eV was used, and reciprocal space was sampled with a density equivalent to at least 192 k-points in the (1×1) surface Brillouin zone. To define the III-V formation enthalpy ΔH_f from the bulk chemical potentials μ^{bulk}, separate DFT calculations were performed for the elements in their ground-state phases: Ga in the α-Ga structure, Al in the face-centered-cubic structure, Sb in the rhombohedral structure, and both AlSb and GaSb in the zinc-blende structure.

III. RESULTS AND DISCUSSIONS

The resulting relative surface energies for AlSb(001) and GaSb(001) are shown in Figs. 3(a) and 3(b), respectively, for
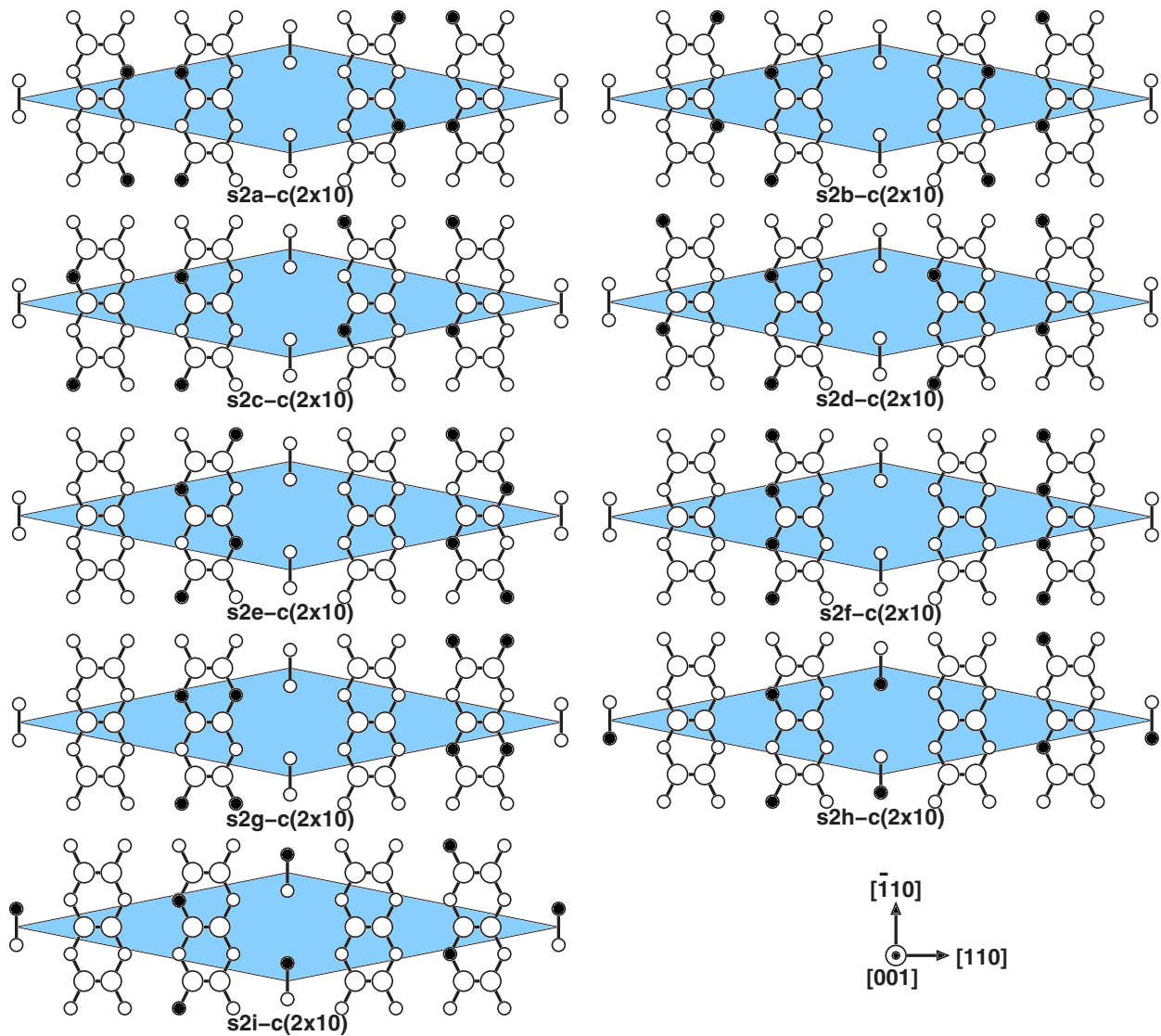
FIG. 5. (Color online) Reconstruction models with a double substitution of Sb atoms by Ga atoms. See Fig. 1 for color schemes.

the eight models considered here. For each model, the surface energy is linear in μ_V, with the slope given by $\Delta\Theta$.

For AlSb(001), the predicted stable reconstructions, and their energetic ordering, are in excellent agreement with experiment. Proceeding from Sb-poor to Sb-rich conditions, the predicted sequence is $\alpha(4\times3)\rightarrow\beta(4\times3)\rightarrow\gamma(4\times3)\rightarrow c(4\times4)$, as reported previously.[13] This is the same sequence observed experimentally.[13] Moreover, $\gamma(4\times3)$ is predicted to exist only over a very narrow range of μ_{Sb}, in agreement with experiment.[13]

For GaSb(001), the predicted sequence is qualitatively the same as for AlSb(001), although the $c(4\times4)$ is only predicted to be stable for values of μ_{Sb} above the thermodynamically allowed limit of zero. Experimentally, however, the situation is quite different. As reported previously, neither the $\gamma(4\times3)$ nor the $c(4\times4)$ phase is observed for any growth condition.[13] Instead, under Sb-rich conditions, only the (1×5) and (2×5) periodicities have been observed.[12]

Righi *et al.* suggested $h0(4\times3)$, shown in Fig. 1, as the model for GaSb(001) surface under these conditions.[24] Our

calculation indeed shows that it is energetically as favorable as $\gamma(4\times3)$, as shown in Fig. 3(b) and in Table I. However, $h0(4\times3)$ must be rejected as it has a wrong periodicity.

In order to explain the experimentally observed (1×5) and (2×5) structures on GaSb(001) surface, we studied a large number of structures based on variations of $c(2\times10)$ and (2×10). We note that $c(2\times10)$ violates the ECM substantially ($\Delta\nu=0.3$), and substitution of Sb atoms in the top layer of the underlying Sb-terminated GaSb(001) surface by Ga atoms can lower the excess electron count. Figure 4 shows the possible reconstructions when a single Sb atom is replaced by a Ga atom. We use the naming convention of $s1x$ to denote a "single substitution," As shown in Table I, all $s1x$ reconstructions indeed have lower excess electron counts.

For completeness, we also considered reconstructions resulting from double substitution of Sb atoms by Ga atoms as shown in Fig. 5. More substitutions, however, were not found to be energetically favorable: Table I shows that the surface energies of these structures are higher than that of $s1x$ reconstructions. We note that for these double substitu-
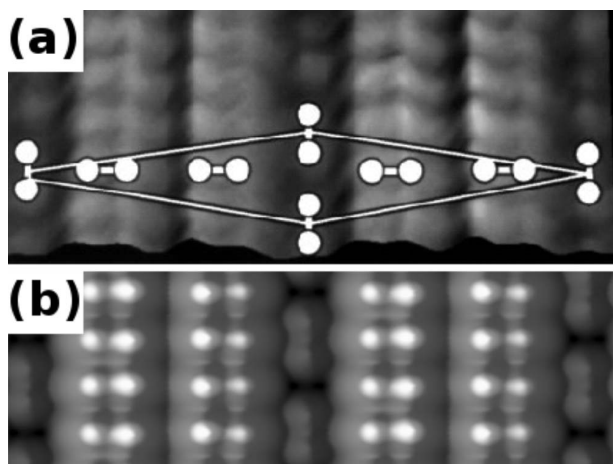
FIG. 6. Filled-state STM images of GaSb(001) with (1×5) periodicity. (a) Experimental STM image; a $c(2\times10)$ unit cell is indicated. (b) Simulated STM image of $s1a-c(2\times10)$. This image shows the asymmetries in the intensities of the current density from two atoms of the horizontal dimers, which were not captured in the simulated STM image of $c(2\times10)$. Compare with Fig. 3(d) of Ref. 12.

tions, the excess electron counts $\Delta\nu$ are negative, indicating a deficit of electrons relative to the ECM.

One of the most energetically favorable structures having the correct periodicity is $s1a-c(2\times10)$, shown in Fig. 4. $s1a-c(2\times10)$ has two clear advantages over $c(2\times10)$. First, the surface energy for $s1a-c(2\times10)$ is lower than that of $c(2\times10)$ by more than 50 meV per (1×1) unit cell. Second, as shown in Fig. 6, the simulated STM image for $s1a-c(2\times10)$ is in a better agreement with the experimental image, in that it reproduces the left-right asymmetry within the surface Sb dimers.[12] Furthermore, as shown in Table I, this model violates the ECM and is thus predicted to be weakly metallic, as observed in tunneling spectroscopy.[25] Therefore, the previously proposed model $c(2\times10)$ is unlikely to be the experimentally realized structure.

However, the calculated surface energy of $s1a-c(2\times10)$ is *higher* than that of $\gamma(4\times3)$, as shown in Table I and Fig. 3(b). Likewise, (2×10), the structural model generally accepted for the surface with (2×5) periodicity, is the least energetically favorable structure among the eight structures of Table I. On the other hand, $\gamma(4\times3)$, the most energetically favorable structure among all the structures considered in this study, has a periodicity that has not been observed experimentally to date. These facts leave us with two possible conclusions: either the correct structural model remains undiscovered or the experimentally obtained surface is not the ground-state structure.

The latter possibility, a kinetically limited surface, bears closer consideration. For example, there may be an activation barrier in forming the mixed dimers on GaSb that cannot be overcome within the growth temperatures and times used here. Indeed, to stabilize these surfaces during the growth, one must go from active growth with both Ga and Sb flux at $\sim500\ ^\circ$C to room temperature and no flux while trying to stabilize the surface. This process typically involved simultaneously lowering the temperature while turning off the Ga and then lowering the Sb flux. The surface cannot be annealed, because that would drive off Sb and create $(n\times3)$ reconstructions. These considerations lead us to propose that the $s1a-c(2\times10)$ structure is the most likely model for the observed GaSb(001) surface as created under Sb-rich growth conditions and subsequently stabilized under vacuum.

IV. SUMMARY AND CONCLUSIONS

We have performed *ab initio* calculations on the surface energy and atomic structure of AlSb(001) and GaSb(001) surfaces with various reconstructions. Surface stability diagrams for a large number of reconstruction models are constructed under different growth conditions. For AlSb(001), we confirmed that the predictions of the currently accepted models are in good agreement with experimentally observed reconstructions. For GaSb(001), we showed that previously proposed model accounts for the experimentally observed reconstructions under Ga-rich growth conditions but fails to explain the experimental observations under Sb-rich conditions. Therefore, we propose $s1a-c(2\times10)$ as a better alternative to existing models for GaSb(001) under extreme Sb-rich growth conditions. Our calculations show that $s1a-c(2\times10)$ has a substantially lower surface energy than all $(n\times5)$-like reconstructions proposed previously and, in addition, it leads to a simulated STM image in better agreement with experiment than existing models. However, $s1a-c(2\times10)$ has higher surface energy than $\gamma(4\times3)$, a model with periodicity that has not been observed. Hence, we conclude that the experimentally observed (1×5) and (2×5) structures on GaSb(001) are not the ground-state structure but the kinetically limited ones.

*kimsg@ccs.msstate.edu

[1] J. B. Boos, W. Kruppa, B. R. Bennett, D. Park, S. W. Kirchoefer, R. Bass, and H. B. Dietrich, IEEE Trans. Electron Devices **45**, 1869 (1998).

[2] J. S. Scott, J. P. Kaminski, S. J. Allen, D. H. Chow, M. Lui, and T. Y. Liu, Surf. Sci. **305**, 389 (1994).

[3] M. J. Yang, W. J. Moore, B. R. Bennett, and B. V. Shanabrook, Electron. Lett. **34**, 270 (1998).

[4] F. Fuchs, U. Weimer, W. Pletschen, J. Schmitz, E. Ahlswede, M. Walther, J. Wagner, and P. Koidl, Appl. Phys. Lett. **71**, 3251 (1997).

[5] Gerhard Klimeck, Roger Lake, and Daniel K. Blanks, Phys. Rev. B **58**, 7279 (1998).

[6] D. Z.-Y. Ting and T. C. McGill, J. Vac. Sci. Technol. B **14**, 2790 (1996).

[7] D. J. Chadi, J. Vac. Sci. Technol. A **5**, 834 (1987).

[8] M. D. Pashley, Phys. Rev. B **40**, 10481 (1989).

[9] John E. Northrup and Sverre Froyen, Phys. Rev. B **50**, 2015 (1994).

[10] S. B. Zhang and Alex Zunger, Phys. Rev. B **53**, 1343 (1996).

[11] C. D. MacPherson, R. A. Wolkow, C. E. J. Mitchell, and A. B. McLean, Phys. Rev. Lett. **77**, 691 (1996).

[12] L. J. Whitman, P. M. Thibado, S. C. Erwin, B. R. Bennett, and B. V. Shanabrook, Phys. Rev. Lett. **79**, 693 (1997).

[13] W. Barvosa-Carter, A. S. Bracker, J. C. Culbertson, B. Z. Nosho, B. V. Shanabrook, L. J. Whitman, Hanchul Kim, N. A. Modine, and E. Kaxiras, Phys. Rev. Lett. **84**, 4649 (2000).

[14] M. T. Sieger, T. Miller, and T.-C. Chiang, Phys. Rev. B **52**, 8256 (1995).

[15] J. Piao, R. Beresford, and W. I. Wang, J. Vac. Sci. Technol. B **8**, 276 (1990).

[16] M. Yano, H. Yokose, Y. Iwai, and M. Inoue, J. Cryst. Growth **111**, 609 (1991).

[17] G. E. Franklin, D. H. Rich, A. Samsavar, E. S. Hirschorn, F. M. Leibsle, T. Miller, and T.-C. Chiang, Phys. Rev. B **41**, 12619 (1990).

[18] Guo-Xin Qian, Richard M. Martin, and D. J. Chadi, Phys. Rev. B **38**, 7649 (1988).

[19] D. M. Ceperley and B. J. Alder, Phys. Rev. Lett. **45**, 566 (1980).

[20] J. P. Perdew and A. Zunger, Phys. Rev. B **23**, 5048 (1981).

[21] D. Vanderbilt, Phys. Rev. B **41**, 7892 (1990).

[22] G. Kresse and J. Hafner, J. Phys.: Condens. Matter **6**, 8245 (1994).

[23] G. Kresse and J. Furthmüller, Phys. Rev. B **54**, 11169 (1996).

[24] M. C. Righi, Rita Magri, and C. M. Bertoni, Phys. Rev. B **71**, 075323 (2005).

[25] R. M. Feenstra, D. A. Collins, D. Z.-Y. Ting, M. W. Wang, and T. C. McGill, Phys. Rev. Lett. **72**, 2749 (1994).